35th Annual International Conference of the IEEE EMBS
Osaka, Japan, 3 - 7 July, 2013

A Surgical Navigation System for Aortic Vascular Surgery: A Practical Approach

M. Uematsu, K. Asato, T. Ichihashi, M. Umezu, R. Nakaoka, A. Matsuoka, S. Aomi, H. Iimura, T. Suzuki, Y. Muragaki, and H. Iseki, *Member, IEEE*

Abstract—**In aortic vascular surgery, a navigation system must represent the anatomical map of individual patient in order to detect the important artery. To provide a proper fit for positions along the dorsoventral axis, the spinous process was added to a currently used anatomical point set consisting of four anterior body landmarks. In addition, we attempted to reduce the registration error by compensating for alignment errors resulting from variations in tissue thickness at each landmark. The alignment values were examined using a human phantom consisting of a skeleton model with subcutaneous tissue in the semilateral position. Using this method, a phantom simulation and five clinical trials were performed. Target errors were evaluated at the orifice of the intercostal artery. In the phantom simulation, the error at the target point was 4.1 ± 2.7 mm. However, for one patient undergoing thoracoabdominal aortic aneurysm replacement surgery, the target error was 8.0 mm using the proposed method.**

I. Introduction

Surgical navigation systems are increasingly employed in various fields of surgery such as neurosurgery, orthopedic surgery, and otological surgery [1], [2]. Furthermore, current research is investigating ways to utilize these systems for minimally invasive surgery [3], [4], which is predicted to become a major form of surgical treatment in the future. However, most surgeries are currently conducted as open surgeries, where the use of these navigation systems is complicated by a large degree of organ deformation.

Cardiovascular surgery still involves a high level of risk. Kuwano et al. [5] reported that approximately 90% of aortic vascular surgeries are performed as open surgeries, during which a connection between the target artery and the vascular graft with sufficient postoperative blood flow is very important for achieving good outcome and avoiding complications. Furthermore, surgeons who perform these surgeries need to have a precise anatomical orientation to identify the location and relations of the target arteries, while excellent skills and abundant experience are also required to make appropriate decisions and ensure patient safety. Therefore, we developed a navigation system for aortic vascular surgery to facilitate better performance by surgeons.

The aim of our study was to develop a reliable system independent of individual variabilities such as skills of the surgeon and body size of the patient. This paper presents our analysis of the registration errors obtained when applying the error alignment method in a human phantom and improvements in the reliability of the navigation system during surgery.

II. Materials and Methods

A. Our navigation system

We used a custom-made surgical navigation system for thoracoabdominal aneurysm surgery. The system was originally developed for brain resection surgery with the aim to avoid damage to critical adjacent structures [6]. Neurosurgical performance has shown improvement with the use of intraoperative MRI. However, thoracoabdominal aortic aneurysm surgery has a strict time constraint. Therefore, as in many traditional systems, preoperative CT images are used to represent the patient's anatomical map.

As shown in Fig. 1, the navigation system consists of a three-dimensional localization sensor (Polaris, NDI), personal computer, monitor, pointing tool, and reference tool. Registration is performed before disinfection, and the reference tool is attached to the bed to measure and compensate for the bed position. During navigation, the positions and orientations of the pointing tool on the patient are tracked by the sensor and projected onto the preoperative CT images and three-dimensional surface models, thus showing anatomical structures in real time.

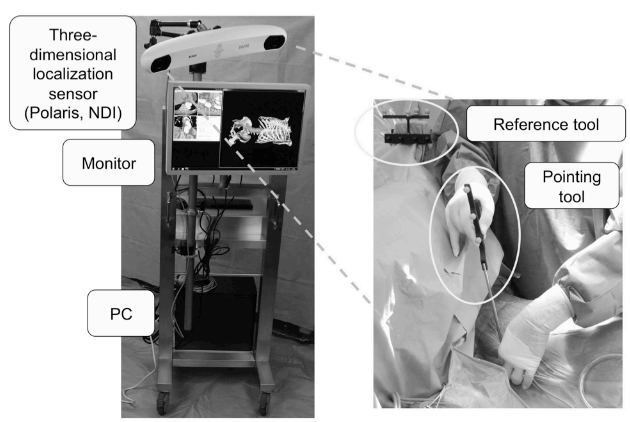

Figure 1. Overview of our navigation system

*Research supported by JSPS KAKENHI 23700590.

M. Uematsu, R. Nakaoka, and A. Matsuoka are with the National Institute of Health Sciences, 1-18-1 Kamiyoga, Setagaya-ku, Tokyo 158-8501, JAPAN (Email: {uematsu, nakaoka, matsuoka}@nihs.go.jp).

K. Asato, T. Ichihashi and M. Umezu are with Waseda University, 3-4-1 Ohkubo, Shinjuku-ku, Tokyo 169-8555, JAPAN (Email: {tmcs108, t.ichihashi}@ruri.waseda.jp, umezu@waseda.jp).

S. Aomi, H. Iimura, T. Suzuki, Y. Muragaki and H. Iseki are with Tokyo Women's Medical University, 8-1 Kawada-cho, Shinjuku-ku, Tokyo 162-8666, JAPAN(Email: {saomi@hij.twmu.ac.jp, imur1149@rad.twmu.ac.jp, {takashi_suzuki, ymuragaki, hiseki}@abmes.twmu.ac.jp).

B. Allowable error of the navigation system for thoracoabdominal aortic aneurysm surgery

In creating a navigation system for aortic vascular replacement surgery, precision of less than 1 mm is difficult to achieve. This is because there are many factors contributing to situational uncertainty, such as the patient's posture, body torsion, and deformation of the aorta.

For our system, the allowable error at the target point is set at 5 mm. In clinical application, it is important to obtain an acceptable level of accuracy for each surgical situation. Figure 2 shows the inner wall of the aorta. The orifices of the arteries are situated within 20 mm of each other. To discriminate the important intercostal artery from its neighbors, a quarter of the distance, that is, 5 mm, should be an acceptable error.

C. Anatomical landmark setting

To match the operation space with the image space, we apply point-based registration using anatomical landmarks that are optimally located in three dimensions. Five points are selected as anatomical landmarks: the jugular notch, sternal angle, pubis, left anterior superior iliac spine, and spinous process (Fig. 3). The jugular notch, sternal angle and pubis crest are all on the same axis. The left anterior superior iliac spine is used to determine the right–left axis [Fig. 3 (a)]. To fit the positions accurately along the dorsoventral axis, the spinous process is added to the four currently used anterior body landmarks [Fig. 3 (b)].

D. Error alignment of tissue thickness

Minimizing measurement errors is important, and these errors depend on the user measuring the positions of the bones from the skin surface. Such values contain errors that depend on the body structure of the patient and the measurement technique of the surgeon.

To estimate the tissue thickness offset, a modeling approach is used to measure the distance of the landmark from the skin. A sheet that mimics human tissue with variable thickness, based on the Shore hardness scale, is placed onto each landmark to form a human phantom (Fig. 4). The values are measured in three orthogonal directions to exactly locate the landmarks with four-pattern thicknesses. The mean and standard deviation are calculated for each measurement to derive the offset value in relation to the tissue thickness.

E. Registration

In this system, the paired-point registration technique is utilized to transform the patient pointing positions from the surgical operational space to the CT image space. The anatomical landmarks $\mathbf{P}_{img}$ are selected in the CT image space by a surgeon who measures the same landmarks $\mathbf{P}_{pat}$ in the patient space. A set of at least three pairs of corresponding points is defined, and the local coordinate systems are calculated using these points. Here ${}^{img}\mathbf{T}_{org}$ expresses the transformation matrix from the world coordinate systems to the image coordinate systems, and ${}^{pat}\mathbf{T}_{org}$ expresses the transformation from the world coordinate systems to the patient coordinate systems. Thus, the transformed point in the CT image space $P'_{i,\,pat\_img}$ is shown by Eq. (1) with a point in the patient space $P_{i,\,pat}$.

$$P'_{i,\,pat\_img} = {}^{img}\mathbf{T}_{pat} \cdot P_{i,\,pat} = {}^{img}\mathbf{T}_{org} \cdot \left({}^{pat}\mathbf{T}_{org}\right)^{-1} \cdot P_{i,\,pat} \qquad (1)$$

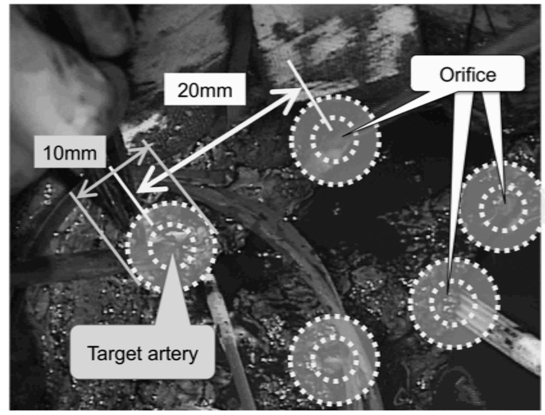

Figure 2. Inside wall of the aorta

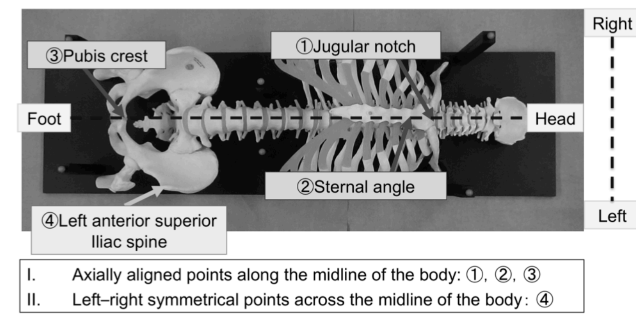

(a) Coronal plane

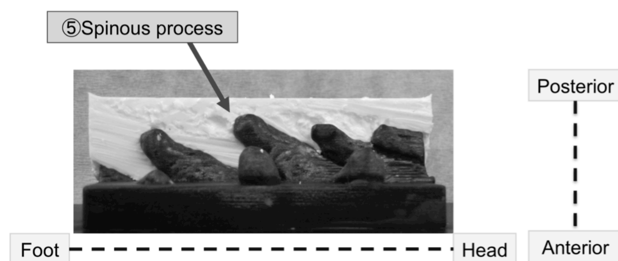

(b) Median sagittal plane

Figure 3. Anatomical landmark setting

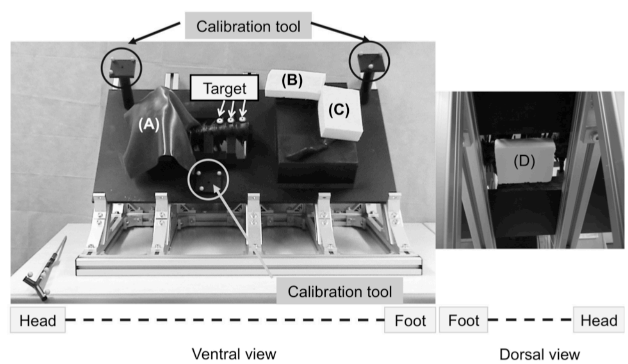

Figure 4. A human phantom with a skin model

F. Evaluation of accuracy by registration errors

Ideally, the location of $P'_{i,\,pat\_img}$ corresponds exactly to $P_{i,\,pat}$. However, they do not have the same values. To evaluate the accuracy of such image-guided navigation system, the following errors are calculated [7], [8].

- The fiducial registration error (FRE) describes how well the geometry of the point pairs defined in the image and patient spaces, respectively, match each other when transformed between spaces.

$$\mathrm{FRE} = \| \mathbf{P}_{img} - {}^{img}\mathbf{T}_{pat} \cdot \mathbf{P}_{pat} \| . \qquad (2)$$

- The target registration error (TRE) is the difference between a target point given in the image space and the same target point given in the patient space transformed with a given registration matrix. TRE represents the true accuracy of the surgical navigation at a given position. Here the target point of the most important artery in the image space is given by $P_{T,img}$ and that in the patient space is given by $P_{T,pat.}$

$$\mathrm{TRE} = \| P_{T,img} - {}^{img}\mathbf{T}_{pat} \cdot P_{T,pat.} \| . \qquad (3)$$

III. Experiments

A. Phantom simulation

Thoracoabdominal vascular surgery is performed in a semilateral position. As shown in Fig. 5, the three-dimensional localization sensor measured anatomical landmarks on the human phantom using the mean tissue thickness obtained from former patients. Twelve individuals measured each landmark five times. FRE and TRE were calculated for four patterns composed of the following factors.

- Landmark selections: (A) four dorsal points, (B) spinous process in addition to A.
- Compensation of tissue thickness: (a) unused, (b) used.

Here fiducial markers were attached to the phantom to indicate the target points. The true values of the target positions were acquired from CT images.

B. Clinical evaluation

Registration was conducted before disinfection. After FRE was calculated, the first navigation was performed to decide the incision lines (Fig. 6). The aorta was exposed after stripping off the outer layer of the pleura. In this process, the second navigation was used to identify the target artery, and a tie marked the artery. After dissecting the aorta, the orifice of the target artery was measured while utilizing the third navigation. Using these data, TRE was calculated. The proposed method (Bb) was applied to five patients and was compared with the conventional method (Aa).

IV. Results

In Figs. 7 to 10, RL denotes right-left, A-P denotes anterior-posterior, and H-F denotes head-foot.

A. Phantom simulation

Figure 7 shows the FRE of phantom simulation. Adding the spinous process increased the error in the anteroposterior direction. The four currently used points were on the same coronal plane, but the dorsal point displaced the plane toward the posterior direction. Thus, the effect was reflected by FRE. On the other hand, no effect of the alignment of tissue thickness was observed.

Figure 8 shows the TRE of the phantom simulation. The error at the target point was reduced from 7.1 ± 3.7 mm using the conventional method (Aa) to 4.1 ± 2.7 mm with our proposed method (Bb). The positions in the craniocaudal direction had an error of less than 5 mm using any method. The alignment of tissue thickness reduced the error for the four-point method, but remained the same for the five-point method.

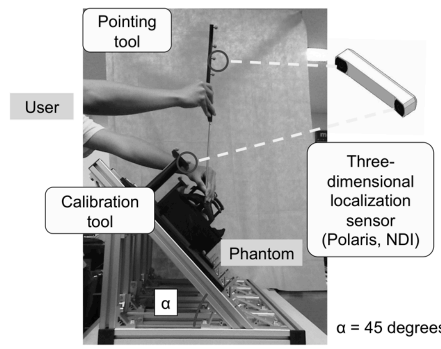

Figure 5. Phantom simulation

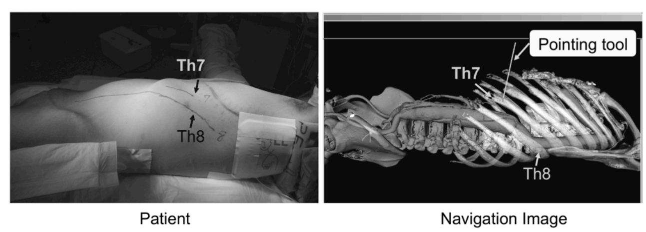

Figure 6. Navigation before thoracotomy

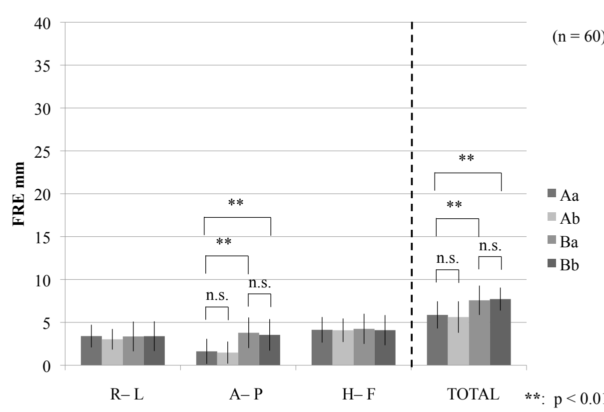

Figure 7. Fiducial registration error (phantom simulation)

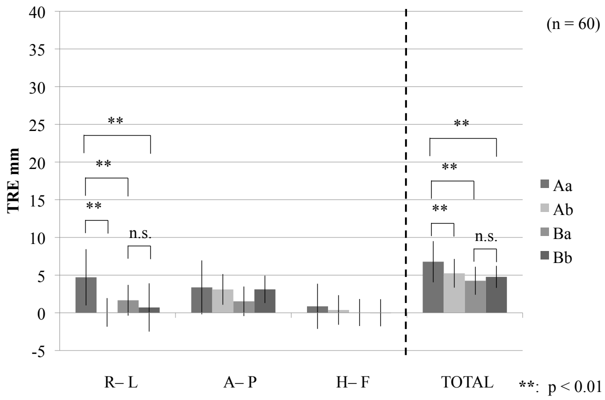

Figure 8. Target registration error (phantom simulation).

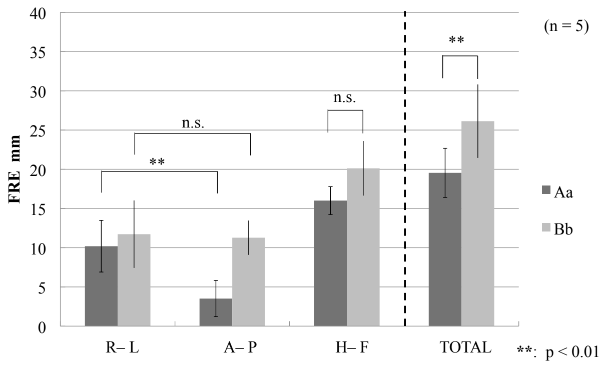

Figure 9. Fiducial registration error (five clinical cases)

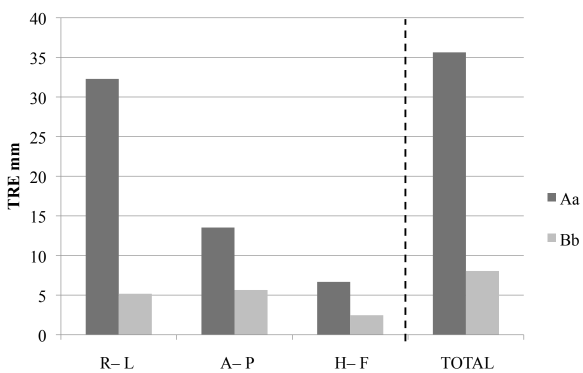

Figure 10. Target registration error (one clinical case)

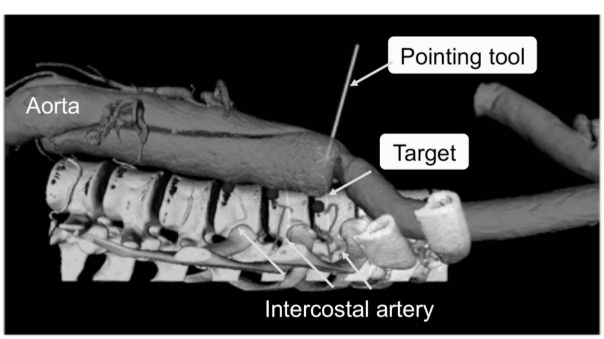

Figure 11. Searching for the target artery using our navigation system

B. *Clinical evaluation*

Figure 9 shows the FRE of clinical evaluation. The errors in clinical cases had the same tendency as in the phantom simulation. However, the magnitude of the errors was larger in the clinical cases than in the phantom simulation. The increase in magnitude of these errors is likely to be caused by variation in patient size.

Figure 10 shows the TRE of clinical evaluation. The error of the target point was reduced from 35.6 mm using the conventional method to 8.0 mm using the proposed method. The positions in almost all directions were less than 5 mm for any method.

Given the time constraint during surgery, measuring the target position in the clinical cases was difficult. Therefore, we show the data of only one clinical case. Our result demonstrates that the navigation guided the target artery well (Fig. 11). Consequently, the surgeon was able to find the most important artery. The navigation system contributed to reducing the stress of the surgeon in performing the procedure. However, the error in this patient is still 8 mm, which is above our proposed allowable error. Further studies are required to examine the source of this error and methods to overcome this issue.

V. CONCLUSION

We conclude that our proposed method improves navigation accuracy in the anteroposterior direction by adding the spinous process as a registration point and by compensating for alignment errors corresponding to the tissue thickness of a patient. In the near future, this method might contribute to identification of target points, enabling surgery without thoracotomy.

REFERENCES

[1] Vector Vision (Brain Lab), http://www.brainlab.com/scripts/website_english.asp

[2] Stealth Station (Medtronic), http://www.medtronicnavigation.com/home

[3] M. J. Mack, “Minimally invasive and robotic surgery,” JAMA, vol. 285, no. 5, pp.568-572, 2001.

[4] D. Burschka, J. J. Corso, M. Dewan, W. Lau, M. Li, H. Lin, P. Marayong, N. Ramey, G. D. Hager, B. Hoffman, D. Larkin, C. Hasser, “Navigating inner space: 3-D assistance for minimally invasive surgery,” Robotics and Autonomous Systems, vol. 52, no. 1, pp.5-26, 2005.

[5] H. Kuwano, J. Amano, H. Yokomine, “Thoracic and cardiovascular surgery in Japan during 2010,” Gen Thorac Cardiovasc Surg, vol. 60, no. nn10, pp.680-708, 2012.

[6] Y. Muragaki, M. Chernov, K. Yoshimitsu, T. Suzuki, H. Iseki, T. Maruyama, M. Tamura, S. Ikuta, M. Nitta, A. Watanabe, T. Saito, J. Okamoto, C. Niki, M. Hayashi, K. Takakura, “Information-guided surgery of intracranial gliomas: overview of an advanced intraoperative technology,” Gen Thorac Cardiovasc Surg, vol. 55, no. 9, pp.377-399, 2007.

[7] J. M. Fitzpatrick, J. B. West, R. Calvin, C. R. Maurer Jr., “Predicting error in rigid-body, point-based registration,” IEEE Trans Med Imag, vol. 17, no. 5, pp.694-702, 1998.

[8] W. Wittmann, T. Wenger, B. Zaminer, T. C. Lueth, “Automatic Correction of Registration Errors in Surgical Navigation Systems,” IEEE Trans Med Imag, vol. 58, no. 10, pp.2922-2930, 2011

[9] J. B. West, J. M. Fitzpatrick, S. A. Toms, C. R. Maurer, Jr, R. J. Maciunas: Fiducial point placement and the accuracy of point-based, rigid body registration,” Neurosurgery, vol. 48, no. 4, pp.810-816, 2001.